HHS Public Access

Author manuscript

*J Orthop Res*. Author manuscript; available in PMC 2018 September 01.

Published in final edited form as:

*J Orthop Res*. 2017 September ; 35(9): 2075–2081. doi:10.1002/jor.23497.

# A Novel Rat Tail Discitis Model Using Bioluminescent *Staphylococcus aureus*

**Phillip A. Bostian**[1], **Jonathan M. Karnes**[1], **Shari Cui**[1], **Lisa J. Robinson**[2], **Scott D. Daffner**[1], **Michelle R. Witt**[2], and **Sanford E. Emery**[1]

[1]Department of Orthopaedics, West Virginia University, P.O. Box 9196, Morgantown, WV 26506-9196

[2]Department of Pathology, West Virginia University, Lab Room 2156, HSC North, Morgantown, WV 26506

## Abstract

Management of spondylodiscitis is a challenging clinical problem requiring medical and surgical treatment strategies. The purpose of this study was to establish a rat model of spondylodiscitis that utilizes bioluminescent *Staphylococcus aureus*, thus permitting *in-vivo* surveillance of infection intensity. Inocula of the bioluminescent *S. aureus* strain XEN36 were created in concentrations of $10^2$ CFU/0.1 mL, $10^4$ CFU/0.1 mL, and $10^6$ CFU/0.1 mL. Three groups of rats were injected with the bacteria in the most proximal intervertebral tail segment. The third most proximal tail segment was injected with saline as a control. Bioluminescence was measured at baseline, 3 days, and weekly for a total of 6 weeks. Detected bioluminescence for each group peaked at day three and returned to baseline at 21 days. The average intensity was highest for the experimental group injected with the most concentrated bacterial solution ($10^6$ CFU/0.1 mL). Radiographic analysis revealed loss of intervertebral disc space and evidence of osseous bridging. Saline injected spaces exhibited no decrease in intervertebral spacing as compared to distal sites. Histologic analysis revealed neutrophilic infiltrates, destruction of the annulus fibrosus and nucleus pulposus, destruction of vertebral endplates, and osseous bridging. Saline injected discs exhibited preserved annulus fibrosus and nucleus pulposus on histology. This study demonstrates that injection of bioluminescent *S. aureus* into the intervertebral disc of a rat tail is a viable animal model for spondylodiscitis research. This model allows for real-time, *in-vivo* quantification of infection intensity, which may decrease the number of animals required for infection studies of the intervertebral disc.

### Keywords

Discitis; Bioluminescence; Infection; Intervertebral Disc; Spine

***Corresponding Author:*** Phillip A. Bostian, MD, Telephone 304-293-1168, Fax Number: 304-293-0231, pabostian@hsc.wvu.edu.

Contribution statement: The study was designed by PB, JK, SC, and SE; data were collected by PB and LR; data were analyzed and processed by PB, JK, SC, LR and SE; the manuscript was written by PB, JK, SC, LR, SD, and SE. All authors have read and approved the final submitted manuscript.

## Introduction

The annual incidence of spondylodiscitis is reported to be 2.2 cases per 100,000[1]. The incidence, however is rising, likely due to a growing number of immunosuppressed patients, an aging population, and the emerging epidemic of intravenous drug abuse[2–4]. The impact of this condition is made worse by the fact that these patients often have a less robust physiologic reserve[5]. Additionally, the indolent and nonspecific course of discitis often delays diagnosis and therefore limits early intervention. As a result, patients hospitalized with this condition have estimated in-hospital mortality rates as high as 10% and average lengths of stay greater than 30 days[6–10]. Despite successful treatment of the infection, these patients exhibit far lower quality of life than that of the general population, and can develop chronic motor and sensory deficits[10; 11]. The combination of a compromised host and an established infection usually requires a protracted treatment course that may include surgical intervention.

Treatment of spondylodiscitis with conventional intravenous antibiotics is often unsuccessful due to restricted drug penetration. The avascular nature of the intervertebral disc leads to an immune privileged environment that permits successful seeding and persistence of bacteria. As a result, successful antimicrobial therapy often requires high dosages for prolonged periods of time. Despite this limitation, antibiotic treatment remains the cornerstone of current spondylodiscitis management[12–14]. Prolonged infections that fail antibiotic treatment often require operative intervention, and thus expose patients to the risks of surgery, increasing the healthcare expenses required for successful treatment.

The medical management of spondylodiscitis has not changed significantly in several decades, and there is substantial potential for the development of novel treatments in this field. Current animal models of spondylodiscitis are technically challenging, requiring paravertebral muscle dissection, intensive anesthesia protocols, and intraoperative fluoroscopy[15–24]. As a result, these models require significant expense to establish infection and require euthanasia of the host specimen to quantify infection intensity. Recently developed animal models of infection have focused on non-invasive methods for the longitudinal quantification of infection intensity, with bioluminescent imaging becoming increasingly more popular[25–27]. The purpose of this study was to develop a preclinical model of spondylodiscitis that reproducibly creates an infection of the intervertebral disc that could be quantified *in-vivo* utilizing bioluminescent *Staphylococcus aureus*. This model obviates the need to euthanize animals at punctuated time points to study therapeutic effects. We hypothesized that inoculation of the *S. aureus* strain XEN36 into the intervertebral disc space of a Sprague-Dawley rat tail would consistently produce a sustained, non-lethal bacterial infection that could be quantified and followed over time using the in-vivo imaging system (IVIS) technology. Here we report successful development of this rat tail spondylodiscitis model that permits real-time monitoring of infection intensity.

## Materials and Methods

### XEN36 Inoculum Preparation

*Staphylococcus aureus* is the most common cause of clinical spondylodiscitis, and therefore we selected a bioluminescent strain of this pathogen for this model. XEN36 *S. aureus* (ATCC 49525 (Perkin Elmer, Waltham, MA)) possesses a Photorhabdus luminescens luxABCDE operon on a native plasmid, which produces a bioluminescent signal. Prior to surgery, a sample of XEN36 stock solution was streaked onto a Remel blood agar plate (Lenexa, KS) and incubated for 18 hours at 37° C. Eighteen hours prior to surgery, 4 colonies of XEN36 were harvested and suspended in 5 mL of brain-heart Infusion (BHI) broth (Becton Dickinson and Co., Franklin Lakes, NJ) and again incubated at 37° C for 18 hours. Immediately prior to inoculation, the samples were centrifuged at 3,000 g for 15 minutes, the solution was decanted, and the pellet was resuspended in 10 mL of phosphate buffered saline without magnesium or calcium (PBS). The sample was subsequently diluted with PBS until an optical density measurement of 0.5 at 600 nanometers (BioMate 3, Thermo Fisher Scientific, Waltham, MA) was obtained, which equates to a concentration of $1.0 \times 10^8$ colony forming units per milliliter (CFU/mL). This sample was then serially diluted with PBS to create three separate inocula with bacterial concentrations of $10^2$ CFU/0.1 mL, $10^4$ CFU/0.1 mL, and $10^6$ CFU/0.1 mL. One hundred microliters (100 μL) of each inoculum was drawn up into 1 mL syringes and stored on ice until time of administration.

### Inoculation of Rat Intervertebral Discs

All animal procedures were approved by our Institutional Animal Care and Use Committee. Adult male Sprague-Dawley rats were purchased from Hilltop Lab Animals, Inc. (Scottdale, PA) and housed in our facility's vivarium under a 12 hour light/dark cycle. Animals were provided access to food and water ad-libitum. Animals were given seven days to acclimate prior to the start of the study. Eighteen animals were randomly divided into the three inoculation groups ($10^2$ CFU/0.1 mL, $10^4$ CFU/0.1 mL, and $10^6$ CFU/0.1 mL). Animals were anesthetized using inhalational isoflurane, and the absence of a corneal reflex was used to confirm sedation. Puralube ointment was applied to both eyes and 5 mg/kg of carprofen was administered for analgesia. Following induction, the proximal tail segment was shaved and the three most proximal intervertebral segments distal to the coat/tail transition were identified using palpation. Calipers were used to measure the diameter at each segment, and half of that distance was transcribed onto the tip of a 27 gauge needle using a sterile marking pen. This measurement was used to approximate the depth of the center of the intervertebral disc. After prepping the injection area twice with an isopropyl alcohol swab, the sterile 27 gauge needle was inserted in the third most proximal segment beginning in the dorsolateral position, taking care not to compromise vascular structures. After the calculated depth was reached, 100 μL of sterile PBS was injected into the nucleus pulposus as a sterile control. When the needle is positioned correctly, fluid flows with minimal resistance into the intervertebral disc. Next, 100 μL of one of the three bacterial concentrations was injected into the most proximal intervertebral disc, leaving a native intervertebral segment between the experimental and control segments.

### In-vivo Monitoring of Infection

The In-Vivo Imaging System (Lumina II, Perkin Elmer, Waltham, MA) and the Living Image software was used to quantify bioluminescence and was expressed in photons/second/centimeter$^2$ (p/sec/cm$^2$). Animals were imaged at 0, 3, 7, 14, 21, 28, 35, and 42 days following injection. For these imaging sessions, animals were anesthetized using the integrated inhalational isoflurane system, and the tails were imaged in a dorsal position. Binning was set to large, field of view was set to D, and the capture time was 5 minutes. Baseline radiance was determined by imaging a non-inoculated rat at the same parameters as the infected rats.

### Histological Analysis

Following euthanasia, three tissue samples of the affected tail segments from each injection group were randomly selected for histological analysis. Using rongeurs and scalpels, longitudinal corticotomies in the included vertebrae were created to allow infiltration of 10% formalin fixative. Samples were decalcified in Histoperfect Rapid Cal decal solution (BBC Biochemical, Mount Vernon, WA) until the bone was easily penetrated with a metal probe. Samples were then processed using 10% formalin, graded alcohols, xylenes, and finally paraffin. They were then prepared on a microtome at 5 microns and dried in a slide warming oven overnight and later stained with hematoxylin and eosin (H&E), safranin-O and fast green, and gram staining.

### Post-Mortem Imaging

At euthanasia, one rat from each group underwent Faxitron radiographic imaging (Model #43805N, Faxitron, Tucson, AZ) to evaluate disc space narrowing and osseous bridging. To evaluate more fully the observed fusion characteristics at the disc segment, two animals inoculated with $10^4$ CFU/0.1 mL (Group 2) inoculum were imaged using microCT (SkyScan 1272, Bruker, Billerica, MA) following euthanasia.

### Statistical analysis

Descriptive statistics, two way analysis of variance (ANOVA), and the Tukey post-test were used to compare the average radiance (p/sec/cm$^2$) emitted between the three groups of animals and for each group at prescribed time points. Significance was set at $p<0.05$.

## Results

### IVIS Imaging

All animals survived until euthanasia and none exhibited signs of systemic infection. At day 0, Group 3 ($10^6$ CFU/0.1 mL) was the only group that exhibited a statistically significant difference in radiance as compared to baseline (9,305 p/sec/cm$^2$ vs. 2,900 p/sec/cm$^2$, $p=0.0026$), but by the third day following injection, all groups exhibited significant increases in radiance from baseline (Group 1 = 12,402 p/sec/cm$^2$, $p<0.0001$; Group 2 = 14,533 p/sec/cm$^2$, $p<0.0001$; Group 3 = 21,033 p/sec/cm$^2$, $p<0.001$) (Figure 1). At one week, all groups continued to demonstrate significant increases in radiance from baseline measurements (group 1 = 8,403 p/sec/cm$^2$, $p=0.0134$; group 2 = 10,278 p/sec/cm$^2$, $p=0.0004$

group 3 = 16,837 p/sec/cm$^2$, p<0.0001). By two weeks, no significant differences were observed in radiance measurements between infected groups and baseline. While radiance measurements between Groups 1 and 2 never differed significantly, Group 3 had statistically higher radiance measurements compared to Groups 1 and 2 on days 0, 3, and 7. Bioluminescence for each group peaked at day 3, and returned to baseline by day 21. Unexpectedly, we noted several specimens that developed bioluminescence in subcutaneous locations extending from the original injection site (Figure 2). Orthogonal IVIS imaging confirmed that this bacterial spread was subcutaneous in location and did not violate adjacent intervertebral disc spaces.

### Histologic results

Samples processed using H&E, safranin-o and fast green, and gram staining were available for analysis (Figure 4). H&E analysis revealed abscess formation defined by a predominantly neutrophilic inflammatory infiltrate. Reactive bone formation in the context of inflammation and repair was noted at the periphery of the intervertebral segments. Safranin-O with fast green counterstain revealed complete destruction of the vertebral endplate and adjacent physis. Gram staining revealed gram positive bacteria retained within abscesses. Of note, bacteria were often found in association with necrotic bone fragments at the core of the abscesses. Staining of control segments revealed preserved structure without endplate disruption or inflammatory infiltration.

### Radiologic results

At euthanasia, the affected vertebral segment was stiff to palpation, and therefore, Faxitron radiographic imaging was performed to qualitatively assess osseous changes (Figure 5). Infected segments showed no clear intervertebral disc space and formation of osteophytes, consistent with evolving, but incomplete osseous bridging. To further assess osseous changes at the affected segments, micro CT scan was performed on two specimens. Images showed incomplete trabecular bridging, destruction of vertebral endplates, and sequestrum formation (Figure 6). Control segments showed no radiographic changes.

## Discussion

Despite a significant lack of consensus over the optimal route, duration, or class of antibiotic, medical management of spondylodiscitis has remained the same for several decades. The increasing number of patients with immunosuppression as well as the growing incidence of antibiotic resistant bacteria emphasizes the expanding need for better conservative management of spondylodiscitis. The present study describes a preclinical model that permits objective, real-time, efficient evaluation of novel therapeutics for the treatment of spondylodiscitis without the need to euthanize the animal to determine the impact on infection.

To our knowledge, this is the first model of spondylodiscitis to use bioluminescent bacteria for the visualization and quantification of intervertebral disc infection. This model has the potential to improve the ability to increase study sample sizes while minimizing expenses of spondylodiscitis studies. Established models of spine infection typically utilize larger

animals and require paravertebral muscle dissection, intraoperative fluoroscopy, and intensive anesthesia protocols[15–24]. Furthermore, these models require euthanasia at specific time points to evaluate infection intensity. These factors increase the number of animals required to execute infection studies, and as a result increase the associated costs of these studies. Because this model uses a simple inoculation procedure and does not require euthanasia to study therapeutic effect over time, the use of bioluminescent bacteria in rat tails could significantly reduce these costs.

In the present study, we simulated spondylodiscitis by injecting *S. aureus* directly into the intervertebral disc. Detected bioluminescence was most intense at 7 days and returned to baseline by 21 days. The decrease in bioluminescence at 21 days was likely due to depletion of the nutrient environment, reduction in bacterial counts secondary to immunologic attack, and sequestration of bacteria by the immune environment. Each group exhibited a spike in bioluminescence between day 3 and 7 followed by a linear decline to baseline at day 21. These findings indicate that seeding of the intervertebral disc is followed by a logarithmic bacterial growth phase. As the infection expands and approaches immunologically active vertebral endplates, planktonic bacteria is eliminated by host defenses. Additionally, bacteria begin to form biofilm and enter a state of senescence, further decreasing the emitted bioluminescent signal[26; 28–31]

Another unique aspect of this model is the use of the rat tail vertebral column for the simulation of spondylodiscitis. This location allows for easier inoculation and clinical evaluation when compared to models that use a more proximal spinal section. Most cases of clinical spondylodiscitis begin secondary to hematogenous seeding of the vertebral endplates by way of metaphyseal arteries[32]. In this model, we injected bacteria directly into the disc to induce infection. While this method of bacterial seeding differs from the pathologic etiology in humans, our tissue analysis demonstrates histologic and radiographic findings similar to clinical spondylodiscitis.

An unexpected finding was that retained bacteria within the core of intervertebral abscesses were nearly always associated with necrotic bone. While we were also able to identify sequestrum formation on micro CT, the finding of necrotic bone in proximity to retained bacteria was distinct. The importance of this finding is as yet unclear, but suggests that necrotic bone fragments might provide shelter for bacteria from immunologic defenses.

It is important to note that there are some limitations to this described model. First, we noted bioluminescence in a subcutaneous location extending from the inoculation site. These findings are consistent with the induction of a soft tissue infection, and is likely due to extravasation of the inoculum from the injection site into surrounding tissues. Future experiments using this model should use a smaller volume of inoculum and a smaller injection needle to limit elution from the intervertebral disc. Second, because an injection was used to introduce bacteria into the intervertebral disc space, the effects of the needle puncture injury on disc architecture were not directly assessed. While established animal models of disc degeneration use annular puncture to induce degeneration, we did not observe these effects in our control segments. Recent studies suggest that the degeneration associated with these injuries is based on needle gauge and that needle sizes similar to the

ones in this study can be used for the delivery of therapeutics to the intradiscal environment without inducing degeneration[33; 34]. Future studies could more fully characterize the degenerative sequelae associated with the needle stick if undisturbed vertebral segments were used as controls. Third, we noted the presence of bacteria at euthanasia despite the lack of detected bioluminescent signal. This is likely due to bacterial counts that do not exceed the threshold required for detection. While the concentrations of bacteria used in this study are relevant for acute spondylodiscitis, this model is unlikely to adequately simulate an indolent infection. Lastly, the present study did not include an interventional arm and, as a result, further investigation is necessary to determine the ability of this model to detect therapeutic effect. Although these are real limitations, histological and radiographic analysis are consistent with a host reaction to spondylodiscitis, supporting the validity of this animal model.

This model might also be enhanced by volumetric micro CT analysis of the tail vertebra as a means to quantify changes in reactive bone formation, loss of intervertebral space, and osteolysis between treated and untreated groups. Our qualitative micro CT analysis demonstrated reactive bone formation and extensive osteolysis of adjacent vertebral endplates. Indeed, prior rodent models of infection have demonstrated the utility of assessing these differences between treatment and control groups as a proxy for therapeutic effect, and quantitative analysis of these bony changes is likely to strengthen this model[26; 37].

Implementation of this model may ease the burden and associated expense of executing preclinical studies of spondylodiscitis and facilitate investigations into antibiotic and novel biologic treatments for the conservative management of spondylodiscitis. Although surgery can be used to eradicate infections that fail medical management, the significant morbidity associated with these procedures as well as the inability of surgery by itself to cure the infection demands better biological interventions. The present study describes a preclinical model that permits objective, real-time, and efficient evaluation of novel therapeutics for the treatment of spondylodiscitis.

## Acknowledgments

We wish to acknowledge the West Virginia University's shared research facilities for imaging assistance and use of the micro CT and IVIS.

PB, SC, and SE have no conflicts of interest to report. JK has received research support from Amniox Medical, Inc. SD owns stocks or stock options in Amgen Co. and Pfizer, receives research support from Bioventus, Pfizer, and Spinal Kinetics, and is on the editorial or governing board of Orthopaedic & Muscular System.

Research reported in this publication was supported by the National Institute of General Medical Sciences of the National Institutes of Health under Award Number U54GM104942. The content is solely the responsibility of the authors and does not necessarily represent the official views of the National Institutes of Health.

## References

1. Beronius M, Bergman B, Andersson R. Vertebral osteomyelitis in Goteborg, Sweden: a retrospective study of patients during 1990–95. Scand J Infect Dis. 2001; 33:527–532. [PubMed: 11515764]
2. Pupaibool J, Vasoo S, Erwin PJ, et al. The utility of image-guided percutaneous needle aspiration biopsy for the diagnosis of spontaneous vertebral osteomyelitis: a systematic review and meta-analysis. Spine J. 2015; 15:122–131. [PubMed: 25058561]

3. Berbari EF, Kanj SS, Kowalski TJ, et al. 2015 Infectious Diseases Society of America (IDSA) Clinical Practice Guidelines for the Diagnosis and Treatment of Native Vertebral Osteomyelitis in Adults. Clin Infect Dis. 2015; 61:e26–46. [PubMed: 26229122]
4. Sur A, Tsang K, Brown M, et al. Management of adult spontaneous spondylodiscitis and its rising incidence. Ann R Coll Surg Engl. 2015; 97:451–455. [PubMed: 26274746]
5. Zarghooni K, Rollinghoff M, Sobottke R, et al. Treatment of spondylodiscitis. International orthopaedics. 2012; 36:405–411. [PubMed: 22143315]
6. Butler JS, Shelly MJ, Timlin M, et al. Nontuberculous pyogenic spinal infection in adults: a 12-year experience from a tertiary referral center. Spine (Phila Pa 1976). 2006; 31:2695–2700. [PubMed: 17077738]
7. Frangen TM, Kalicke T, Gottwald M, et al. Surgical management of spondylodiscitis. An analysis of 78 cases. Unfallchirurg. 2006; 109:743–753. [PubMed: 16897028]
8. Linhardt O, Matussek J, Refior HJ, et al. Long-term results of ventro-dorsal versus ventral instrumentation fusion in the treatment of spondylitis. Int Orthop. 2007; 31:113–119. [PubMed: 16708233]
9. Isenberg J, Jubel A, Hahn U, et al. Multistep surgery for spondylosyndesis. Treatment concept of destructive spondylodiscitis in patients with reduced general condition. Orthopade. 2005; 34:159–166. [PubMed: 15480543]
10. Woertgen C, Rothoerl RD, Englert C, et al. Pyogenic spinal infections and outcome according to the 36-item short form health survey. J Neurosurg Spine. 2006; 4:441–446. [PubMed: 16776354]
11. Lerner T, Hackenberg L, Rosler S, et al. Surgical therapy of unspecific and specific Spondylodiscitis. Z Orthop Ihre Grenzgeb. 2005; 143:204–212. [PubMed: 15849640]
12. Duarte RM, Vaccaro AR. Spinal infection: state of the art and management algorithm. European spine journal: official publication of the European Spine Society, the European Spinal Deformity Society, and the European Section of the Cervical Spine Research Society. 2013; 22:2787–2799.
13. Gouliouris T, Aliyu SH, Brown NM. Spondylodiscitis: update on diagnosis and management. The Journal of antimicrobial chemotherapy. 2010; 65(Suppl 3:iii):11–24.
14. Grados F, Lescure FX, Senneville E, et al. Suggestions for managing pyogenic (non-tuberculous) discitis in adults. Joint Bone Spine. 2007; 74:133–139. [PubMed: 17337352]
15. Chen WH, Jiang LS, Dai LY. A novel canine model of acute pyogenic spondylodiscitis. Neurosurg Rev. 2009; 32:485–490. [PubMed: 19603207]
16. Chen WH, Kang YJ, Dai LY, et al. Bacteria detected after instrumentation surgery for pyogenic vertebral osteomyelitis in a canine model. Eur Spine J. 2014; 23:838–845. [PubMed: 24121752]
17. Koh S. Development and progression of pyogenic spondylitis in a canine experimental model. Nihon Seikeigeka Gakkai Zasshi. 1995; 69:1004–1013. [PubMed: 8551086]
18. Zhang L, Wang JC, Feng XM, et al. Antibiotic penetration into rabbit nucleus pulposus with discitis. Eur J Orthop Surg Traumatol. 2014; 24:453–458. [PubMed: 24043368]
19. Bierry G, Jehl F, Prevost G, et al. Percutaneous inoculated rabbit model of intervertebral disc space infection: magnetic resonance imaging features with pathological correlation. Joint Bone Spine. 2008; 75:465–470. [PubMed: 18485785]
20. Conaughty JM, Chen J, Martinez OV, et al. Efficacy of linezolid versus vancomycin in the treatment of methicillin-resistant Staphylococcus aureus discitis: a controlled animal model. Spine (Phila Pa 1976). 2006; 31:E830–832. [PubMed: 17047530]
21. Guiboux JP, Cantor JB, Small SD, et al. The effect of prophylactic antibiotics on iatrogenic intervertebral disc infections. a rabbit model. Spine (Phila Pa 1976). 1995; 20:685–688. [PubMed: 7604344]
22. Szypryt EP, Hardy JG, Hinton CE, et al. A comparison between magnetic resonance imaging and scintigraphic bone imaging in the diagnosis of disc space infection in an animal model. Spine (Phila Pa 1976). 1988; 13:1042–1048. [PubMed: 3206298]
23. Walters R, Rahmat R, Shimamura Y, et al. Prophylactic cephazolin to prevent discitis in an ovine model. Spine (Phila Pa 1976). 2006; 31:391–396. [PubMed: 16481948]
24. Yucesoy K, Ozer E, Gulay Z, et al. Histopathologic effects of discitis on neural tissues: an experimental study. J Spinal Disord Tech. 2004; 17:112–114. [PubMed: 15260093]

25. Funao H, Ishii K, Nagai S, et al. Establishment of a real-time, quantitative, and reproducible mouse model of Staphylococcus osteomyelitis using bioluminescence imaging. Infect Immun. 2012; 80:733–741. [PubMed: 22104103]
26. Inzana JA, Schwarz EM, Kates SL, et al. A novel murine model of established Staphylococcal bone infection in the presence of a fracture fixation plate to study therapies utilizing antibiotic-laden spacers after revision surgery. Bone. 2015; 72:128–136. [PubMed: 25459073]
27. Walton KD, Lord A, Kendall LV, et al. Comparison of 3 real-time, quantitative murine models of staphylococcal biofilm infection by using in vivo bioluminescent imaging. Comp Med. 2014; 64:25–33. [PubMed: 24512958]
28. Nishitani K, Sutipornpalangkul W, de Mesy Bentley KL, et al. Quantifying the natural history of biofilm formation in vivo during the establishment of chronic implant-associated Staphylococcus aureus osteomyelitis in mice to identify critical pathogen and host factors. J Orthop Res. 2015; 33:1311–1319. [PubMed: 25820925]
29. Li D, Gromov K, Soballe K, et al. Quantitative mouse model of implant-associated osteomyelitis and the kinetics of microbial growth, osteolysis, and humoral immunity. J Orthop Res. 2008; 26:96–105. [PubMed: 17676625]
30. Pribaz JR, Bernthal NM, Billi F, et al. Mouse model of chronic post-arthroplasty infection: noninvasive in vivo bioluminescence imaging to monitor bacterial burden for long-term study. J Orthop Res. 2012; 30:335–340. [PubMed: 21837686]
31. Sun Z, Zhang M, Zhao XH, et al. Immune cascades in human intervertebral disc: the pros and cons. Int J Clin Exp Pathol. 2013; 6:1009–1014. [PubMed: 23696917]
32. Wiley AM, Trueta J. The vascular anatomy of the spine and its relationship to pyogenic vertebral osteomyelitis. J Bone Joint Surg Br. 1959; 41-b:796–809. [PubMed: 13855377]
33. Zhang H, La Marca F, Hollister SJ, et al. Developing consistently reproducible intervertebral disc degeneration at rat caudal spine by using needle puncture. J Neurosurg Spine. 2009; 10:522–530. [PubMed: 19558284]
34. Martin JT, Gorth DJ, Beattie EE, et al. Needle puncture injury causes acute and long-term mechanical deficiency in a mouse model of intervertebral disc degeneration. J Orthop Res. 2013; 31:1276–1282. [PubMed: 23553925]
35. Raymond CR, Conlan JW. Differential susceptibility of Sprague-Dawley and Fischer 344 rats to infection by Francisella tularensis. Microb Pathog. 2009; 46:231–234. [PubMed: 19490832]
36. Cacioppo LD, Shen Z, Parry NM, et al. Resistance of Sprague-Dawley Rats to infection with Helicobacter pullorum. J Am Assoc Lab Anim Sci. 2012; 51:803–807. [PubMed: 23294887]
37. Green JM, Hallab NJ, Liao YS, et al. Anti-oxidation treatment of ultra high molecular weight polyethylene components to decrease periprosthetic osteolysis: evaluation of osteolytic and osteogenic properties of wear debris particles in a murine calvaria model. Curr Rheumatol Rep. 2013; 15:325. [PubMed: 23532463]

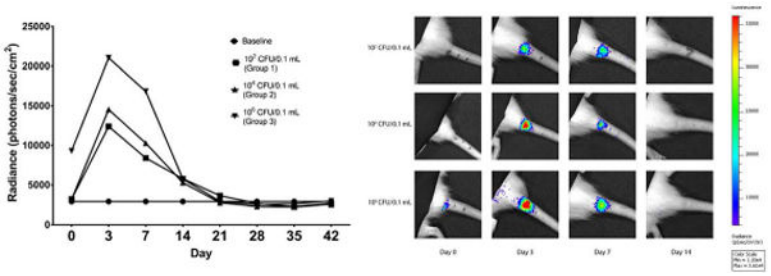


**Figure 1.**

Bioluminescent results over time. Radiance returned to baseline by day 21 (left). Radiance intensity overlaid on grayscale image of subjects (right).

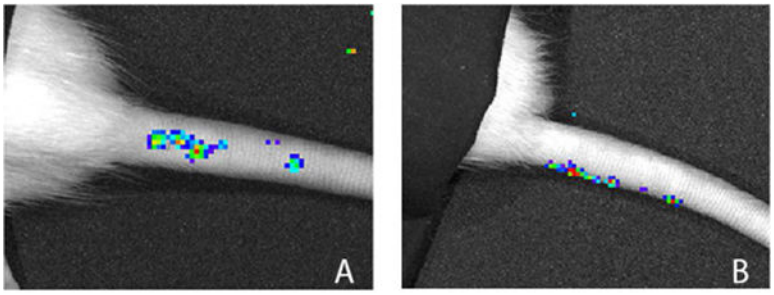


**Figure 2.**
Bioluminescent intensity map demonstrating subcutaneous spread of bacteria from site of inoculation (A). Orthogonal imaging revealed that this signal originates from a subcutaneous position (B).

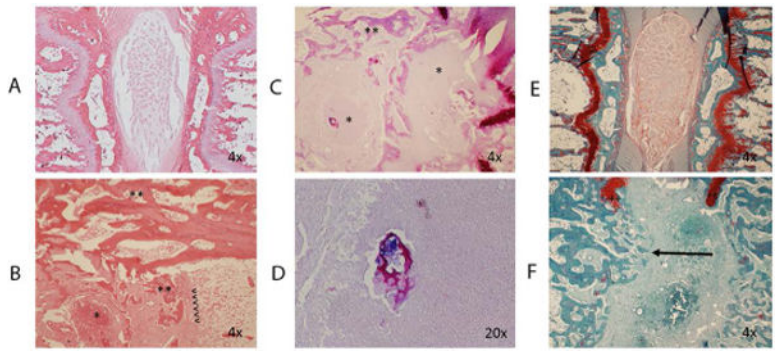


**Figure 3.**

A: H&E staining of control intervertebral segments. Normal architecture is preserved. B: H&E staining of infected intervertebral segment. Reactive bone formation (**), and abscess (*) are noted. Original position of endplate is noted (<). C: Gram staining of infected segment demonstrates abscesses (*) and reactive bone formation (**). D: Gram stain demonstrates bacteria in proximity to necrotic bone. E: Safranin-O and fast green staining of the control disc. F: Safranin-O staining of infected disc demonstrating endplate destruction and trabecular bridging (arrow). Remnants of the cartilaginous endplate are noted (++).


**Figure 4.**
Faxitron imaging of infected and uninfected segments. No intervertebral space is noted at the infected area (arrow).

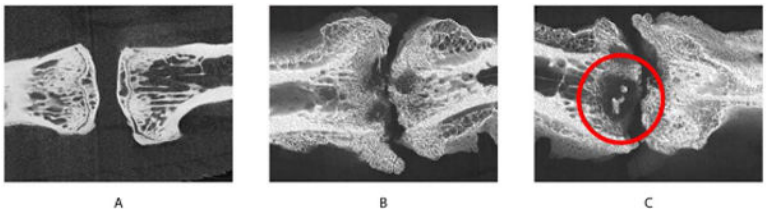


**Figure 5.**

Micro CT images of uninfected (A) and infected (B & C) segments. Reactive bone formation is noted at the periphery of the infected segments. Partial trabecular bridging is also noted. Sequestrum formation is evident near the endplate (C).

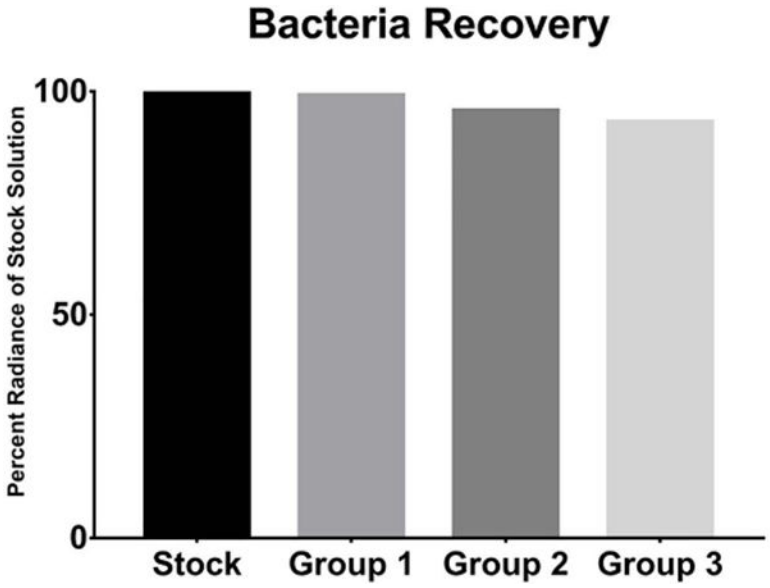


**Figure 6.**

Percent radiance of recovered bacteria compared to stock solution. No significant differences noted between groups.